

# Emergent quasiparticles in Euclidean tilings

F. Crasto de Lima \* and A. Fazzio †

Brazilian Nanotechnology National Laboratory CNPEM,  
C.P. 6192, 13083-970, Campinas, SP, Brazil

(Dated: November 26, 2020)

Material's geometrical structure is a fundamental part of their properties. The honeycomb geometry of graphene is responsible for the arising of its Dirac cone, while the kagome and Lieb lattice hosts flat bands and pseudospin-1 Dirac dispersion. These features seem to be particular for few 2D systems rather than a common occurrence. Given this correlation between structure and properties, exploring new geometries can lead to unexplored states and phenomena. Kepler is the pioneer of the mathematical tiling theory, describing ways of filing the euclidean plane with geometrical forms in its book *Harmonices Mundi*. In this letter, we characterize 1255 lattices composed of the euclidean plane's k-uniform tiling, with its intrinsic properties unveiled — this class of arranged tiles present high-degeneracy points, exotic quasiparticles, and flat bands as a common feature. Here, we present aid for experimental interpretation and prediction of new 2D systems.

One question that arises is how to describe all the possible perfectly flat 2D materials? Commonly, we consider real materials formed by entities (orbitals, closed boundaries, waveguides) pinpointing a lattice site, while lines can connect those sites indicating a pair interaction (for instance, as chemical bonds). A precise way to represent such lattices is to tile the Euclidean plane with regular polygons. Such an assumption allow us to describe most of the observed 2D systems, from translational periodic [1] to quasicrystal structures [2]. Their composing types of vertexes can classify the tiling. There are only 21 types of vertexes (encounter of three or more polygons) composed of regular polygons. Considering translational periodicity, 15 from the 21 possible vertexes can tile the plane [3], which are shown in Fig. 1a.

An infinite number of lattices arise combining different vertexes. We can classify such lattices concerning the type of vertexes they are composed, and if these sites are equivalent by crystal symmetry operations. A arrange of tiles composed of regular polygons containing k non-equivalent vertexes is denoted as k-uniform tiling. Interestingly, the most popular synthesized 2D materials are described by the k-uniform tiling. Besides the graphene honeycomb and the kagome lattice, we clarify in Fig. 1c that k=3 tilings describe 2D borophene phases. Exotic fermions can emerge in this systems, for instance, as shown in Fig. 1b, the spin-1/2 Dirac cone of graphene, the flat band of the kagome lattice, and the pseudospin-1 Dirac of the square-octagonal lattice. The characterization of all possible k-uniform tiling is still an open mathematical problem. However, up to k=6, all possible tilings have been found, together with a few k=7, totaling 1255 classified k-uniform tilings [4].

Besides monoatomic materials exploration [5] and its natural discovery, rational design approaches allow precise systems. Currently, we are facing combined efforts between theoretical and experimental groups to realize new 2D materials. For instance, in rational designed metal-organic frameworks, that allow for a tiling based

filing of the plane [6]. Additionally, by varying molecules and annealing process, many structures have been constructed in molecular self-assembly [7–9]. Scanning Tunneling Microscopy (STM) designed surface crystals allows higher control over the lattice formation [10–13], expanding the capability of lattices exploration. Such high control can also be found in photonic crystals [14], vibroacoustic materials [15, 16], and circuit lattices [17]. Exploring the beam shape techniques such lattices can also be constructed with highly ordered structures in cold-atoms [10], and projecting superlattices directly over 2D materials [18].

A similar problem arises when describing dispersive eigenstates in periodic (i) classical system, for instance, in elastic media or gyroscopic lattices (mass lumped-parameter system), or even (ii) circuit lumped-parameter systems; (iii) electronic crystals, (iv) photonic crystals or (v) cold-atoms in optical lattices. We can describe those systems as quasiparticles moving in periodic lattices. Ultimately we are dealing with an eigenvalue problem of localized elements coupled through some terms. In this letter, we have characterized the energy dispersion of the arising quasiparticles. We consider each vertex of the tiling structure representing a localized entity (orbital, mass, atom, wave) while each edge represents the nearest-neighbor (NN) interaction between these entities. Therefore, a similar hamiltonian structure will be applicable in each particular case. Taking the electronic system as a case of study, we can write

$$H = \sum_{ij} (1 - \delta_{ij}) t_{ij} c_i^\dagger c_j, \quad (1)$$

where  $c_i/c_i^\dagger$  are the annihilation/creation operators of a electron in the  $i$ th site;  $(1 - \delta_{ij})$  sets all on-site energies to zero; and  $t_{ij}$  describes the rate of  $i \rightarrow j$  site transition, i.e. the hoping strength of an electron going from  $i$ th to the  $j$ th site. If we focus on planar isotropic entities, i.e.,  $s$ ,  $p_z$ ,  $d_{z^2}$  orbitals for the electronic case,  $t_{ij}$  assume a simpler distance dependence between  $i$ th and  $j$ th site  $t_{ij} =$

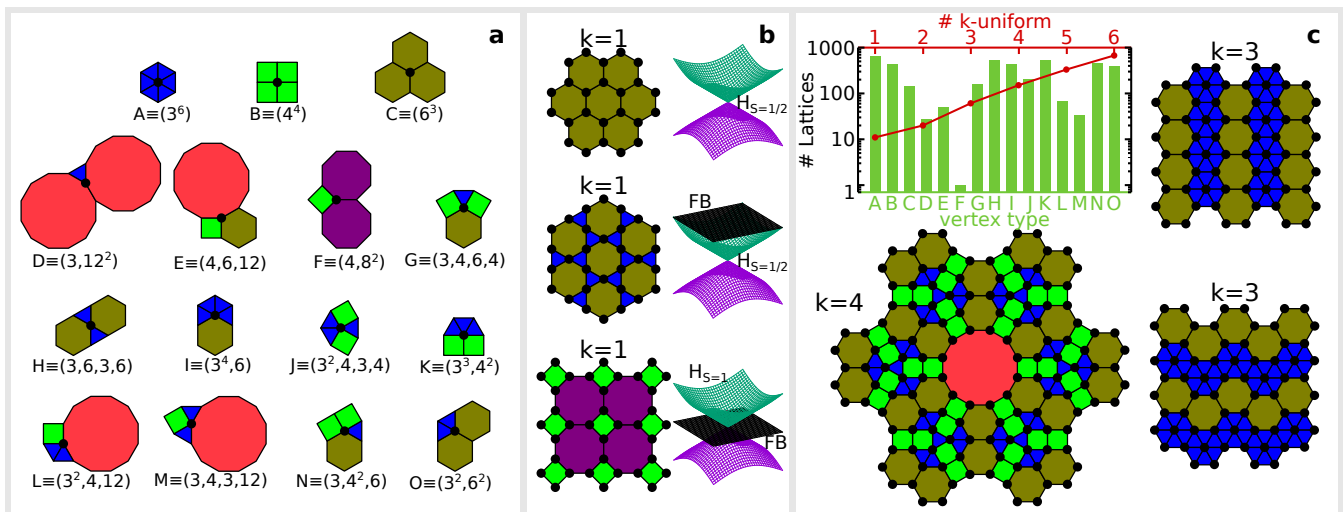


FIG. 1. **Lattices with  $k$  non-equivalent vertex.** **a.** All possible vertex for translational invariant uniform Euclidean tilings, labeled according to conventional notation [3]. **b.** Examples of  $k=1$  uniform tiling and arising quasiparticles. **c.** Graph showing the number of lattices with  $k$  non-equivalent vertices (red) and the number of lattices with at least one vertex of type (green) indicated in **a**, together with three tiling examples.

$t_{ij}(d_{ij})$ . We can parametrize such interaction concerning the NN distance ( $d_{nn}$ ),  $t_{ij} = t \exp[-\alpha(d_{ij} - d_{nn})]$ , in such a way that if  $\alpha \gg d_{nn}^{-1}$  only NN hopping is significant, while for  $\alpha \sim d_{nn}^{-1}$  further neighbors interaction become relevant. Such representation has shown to capture the essence of many materials, for instance, the graphene Dirac cone [19], MOF kagome structures [20], and other 2D systems [21]. In the reported results we have taken  $t = 1$ ,  $d_{nn} = 1$ ,  $\alpha \rightarrow \infty$  for the NN hopping only system, and  $\alpha = 5/d_{nn}$  (unless otherwise stated) for the long-range (LR) coupling. The detailed lattices structure and band dispersion are present in the supplementary information. Here, it is worth emphasizing that LR coupling englobes more than the next-nearest neighbor (NNN) hopping, and taking  $\alpha = 5/d_{nn}$  leads to the reasonable value for the NNN hopping fraction of graphene  $\exp[-5(d_{nnn} - d_{nn})/d_{nn}] \sim 0.03$  [19].

An astonishing feature arising in these  $k$ -uniform tiling is high-degeneracy points. Spacegroup symmetries alone (wallpaper group in 2D case) can predict only 3-fold (2-fold) degeneracies in spinless systems. However, here we found up to 14-fold degeneracy points. Such points predicted here, rather than being accidental [22], are protected by site permutation symmetries [23]. Higher degeneracy points are usually associated with emergent phenomena in materials. For example, supercollimation [24], Klein tunneling [25], Weyl points [26], and from an applied point of view with enhanced thermoelectricity [27]. Although the appealing emergent phenomena, few systems have been shown to provide high-degeneracy points, particularly for higher-pseudospin Dirac effective quasiparticles. Here, 519 lattices host at least one 3-fold degeneracy point from which 119 are robust against

long-range coupling, as shown in Fig. 2a. We can see an almost exponential decaying of the number of lattices hosting a given degeneracy order within the  $k$ -uniform tiling for  $k \leq 7$ . Including long-range coupling can break degeneracies; however, a considerable number of lattices retain such points. For instance, we find 18 lattices hosting 6-fold, while one lattice host a 9-, 10- and 11-fold robust degeneracy.

Remarkably, these degeneracy points can lead to new quasiparticles in condensed matter systems that do not have high-energy counterparts. For instance, the pseudospin- $S$  Dirac fermions described by higher-order Dirac equation  $H_S = \vec{\sigma}_S \cdot \vec{k}$ , where  $\vec{\sigma}_S$  denotes the spin  $S$  angular momentum matrix. For  $S = 1/2$ ,  $\vec{\sigma}_{1/2}$  becomes the Pauli matrix-vector, and the Hamiltonian describes the Dirac fermion present in graphene. In general, for a half-integer spin ( $S = (2n + 1)/2$ ), such an equation describes a set of  $m = n + 1$  degenerated Dirac cones. In contrast, for integer spin ( $S = m$ ), the set  $m$  of Dirac cones further degenerate with an additional flat band. In Fig. 2c we see that the found 14-fold point is composed of eight linear dispersive bands (four Dirac cones), five flat bands and, one quadratically dispersive band along the  $\Gamma$ -M direction. Among the studied lattices, we have classified the number of lattices hosting at least  $m$  Dirac cones (DC), or  $m$  Dirac cones degenerated with at least one flat-band or non-linear dispersive band (DC+). As shown in Fig 2b, similar exponential decaying of the number of lattices with the increase of degeneracy order is seeing.

The arising degeneracy points have a rich diversity in their dispersions. In Fig. 2d we shown a lattice with a pseudospin-1 Dirac quasiparticle [Fig. 2h panel I], but

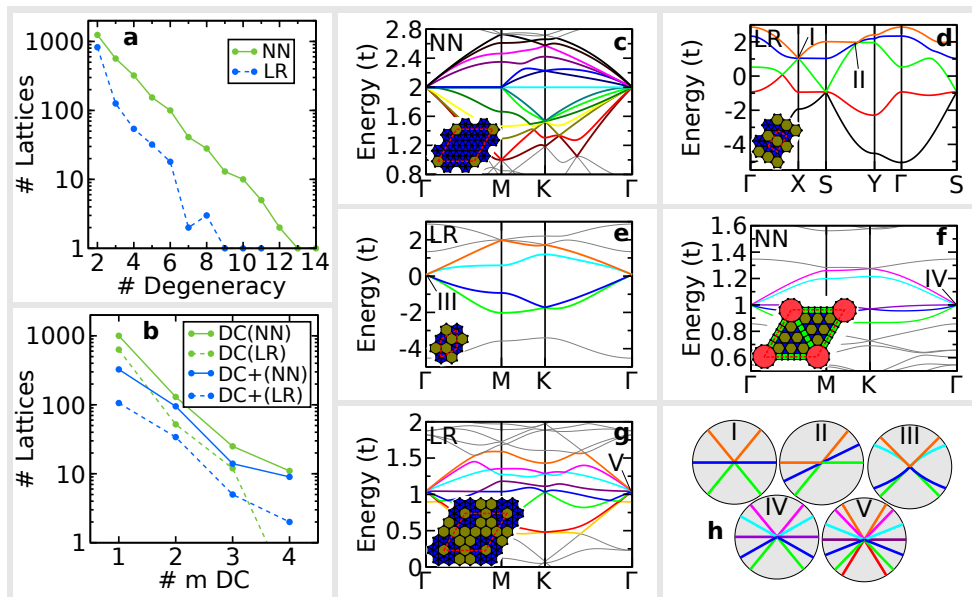


FIG. 2. **Degeneracy points and Dirac cones.** **a.** Number of lattices with at least one point with a given degeneracy order. **b.** Number of lattices with  $m$  degenerated Dirac cones (DC) and  $m$  Dirac cones further degenerated with another non-linear band (DC+). Example of lattices hosting **c.** a 14-fold, **d.** two 3-fold, **e.** a 4-fold, **f.** a 5-fold, and **g.** a 7-fold degeneracy point. **h.** Zoom in the marked degeneracies of the example lattices.

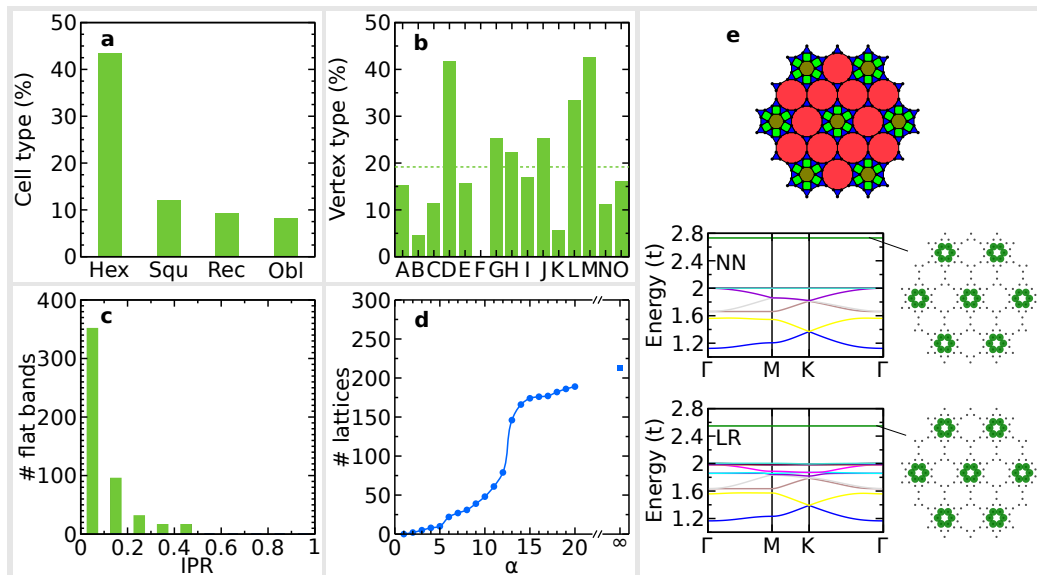


FIG. 3. **Flat bands in k-uniform tiling.** **a.** Percentage of hexagonal, square, rectangular, and oblique lattices with at least one flat band. **b.** Percentage of vertex type of lattices with at least one flat band. **c.** Inverse participation rate of the flat bands. In **a-c** the results are with NN coupling. **d.** The observed number of lattices with flat bands as a function of the long-range factor  $\alpha$ . **e.**  $k=4$  lattice hosting a flat band robust against long-range coupling.

also a 3-fold type-II like Dirac dispersion [Fig. 2h panel II]. This lattice is one of the 106 lattices hosting an LR robust point formed by Dirac cone degenerated with an additional band (DC+ with  $m=1$  in Fig. 2b). It is worth pointing out that no correlation between the vertex types of the lattices and the high-degeneracy points are present. Rather than being local dependent, such de-

generacies are a collective effect of the lattice sites. For instance, as shown in the lattice of Fig. 2f, composed of 5 different types of vertexes, a 5-fold pseudospin-2 Dirac [Fig. 2h panel IV] arises. Focusing on vertex composed of triangles and hexagons [A, C, H, I, and O of Fig. 1a] which leads to triangular based systems, as the ones constructed in controlled STM atomic positioning [13], dif-

ferent quasiparticles can be designed. Besides the 14-fold and 3-fold degeneracy of Figs. 2c and d, in Fig. 2e and f we highlight a 4-fold pseudospin-3/2 Dirac dispersion [Fig. 2h panel III] and a 7-fold pseudospin-3 Dirac quasiparticle [Fig. 2h panel V], respectively. The common appearance of such degenerated Dirac cones in the k-uniform tiling opens opportunities to conetronics manipulations [28].

Together with the Dirac quasiparticle's attention in graphene, we see a grown interest in electronic flat bands. They have emerged as an alternative for high-temperature fractional quantum Hall phase without an external magnetic field [29]. The flatness of the band defines an energy scale to which other effects can compete. For a perfect flat band, any weak perturbation can have a relevant energy contribution. As a consequence, flat bands arising in the condensed matter have shown to present unconventional magnetism [30], superconductivity [31, 32], and a slow light behavior [33].

A given band was considered flat when its dispersion (bandwidth) were lower than  $10^{-4}t$ . For NN coupling, perfect flat bands arise (null bandwidth), for instance, as in the kagome case Fig. 1b. Indeed, for NN coupling, 213 lattices hosting at least one flat band are present among the studied tilings. Those flat bands occur mostly within hexagonal systems, as shown in Fig 3a. Here, 43% of all hexagonal tilings have at least one flat band. The same is true for around 10% in other cells. The correlation between geometry and the presence of flat bands can also be observed among the different lattice vertexes, Fig. 3b. More than 40% of lattices with at least one D or M vertex [Fig. 1a] and more than 30% with L vertex present flat bands. Indeed, comparing the average vertex percentage, the green dashed line of Fig. 3b, indicates that some vertex types have a stronger correlation with the appearance of flat bands.

To show the delocalization nature of the flat band, we calculate the inverse participation rate (IPR)

$$P^{-1} = \left( N \sum_i |\Psi_i|^4 - 1 \right) / (N - 1) \quad (2)$$

with,  $\Psi_i$  the orbital projected wave function and N the lattice's number of sites. The inversion participation rate is bounded to  $0 \leq P^{-1} \leq 1$ , being  $P^{-1} = 1$  a fully localized state, and  $P^{-1} = 0$  a fully delocalized state. In Fig. 3c we shown the number of flat band states within all the 1255 tilings with  $P^{-1}$  within intervals of 0.1. Our results show that these flat bands are delocalized, instead of coming from lone pairs, with most of such states with  $P^{-1} < 0.1$ .

The picture presented above of structural correlation and delocalized IPR is preserved considering LR couplings. However, LR interaction couples flat band states from neighboring cells leading to a dispersive state. In Fig. 3d the number of flat bands for a given LR param-

eter  $\alpha$  is presented. Up to  $\alpha = 14/d_{nn}$  more than 150 lattices preserves the flat band character. The transition observed around  $\alpha = 13/d_{nn}$  can be understood as 70% of the lattices have the next-nearest neighbor (NNN) distance being  $d_{nnn} = \sqrt{2}d_{nn}$ , while 30% with  $d_{nnn} = \sqrt{3}d_{nn}$ . Therefore in such a point, the shorter  $d_{nnn}$  lattices have significant LR interaction while the longer  $d_{nnn}$  is still two orders of magnitude lower. Impressively, increasing such coupling range to  $\alpha = 5/d_{nn}$ , ten lattices still host a flat band. As shown in Fig 3e for one of those lattices, the preserved flat band arises from orbitals further separated from its periodic images. Therefore an even higher coupling range is required for the flatness disappearance.

The controlled experimental realization of different lattices has recently grown in photonic, STM molecular positioning, cold-atoms, and other systems. They allow a rich playground for the exploration of new phenomena in exotic dispersive bands. Here we have shown that, rather than being a rare feature, such states vastly occur among the k-uniform tilings. Indeed, we have predicted here higher pseudospin Dirac points, until now hidden from possible realizations. Our theoretical approach can be broadly interpreted within different systems. The explored systems unveil a class of systems to which we give a guide for experimental lattice construction and data interpretation.

## ACKNOWLEDGMENTS

The authors acknowledge financial support from the Brazilian agencies FAPESP (grants 19/20857-0 and 17/02317-2).

---

\* felipe.lima@lnnano.cnpem.br

† adalberto.fazzio@lnnano.cnpem.br

- [1] Yinghua Jin, Yiming Hu, and Wei Zhang, "Tessellated multiporous two-dimensional covalent organic frameworks," *Nature Reviews Chemistry* **1**, 0056 (2017).
- [2] L. A. Bursill and Peng Ju Lin, "Penrose tiling observed in a quasi-crystal," *Nature* **316**, 50–51 (1985).
- [3] Branko Grünbaum and Geoffrey C. Shephard, "Tilings by Regular Polygons," *Mathematics Magazine* **50**, 227–247 (1977).
- [4] <http://w3.impa.br/~cheque/tiling/>.
- [5] Nicholas R. Glavin, Rahul Rao, Vikas Varshney, Elisabeth Bianco, Amey Apte, Ajit Roy, Emilie Ringe, and Pulickel M. Ajayan, "Emerging Applications of Elemental 2D Materials," *Advanced Materials* **32**, 1904302 (2020).
- [6] Rong-Ran Liang, Shun-Qi Xu, Lei Zhang, Ru-Han A, Pohua Chen, Fu-Zhi Cui, Qiao-Yan Qi, Junliang Sun, and Xin Zhao, "Rational design of crystalline two-dimensional frameworks with highly complicated topo-



- logical structures,” *Nature Communications* **10**, 4609 (2019).
- [7] Fang Cheng, Xue-Jun Wu, Zhixin Hu, Xuefeng Lu, Zijing Ding, Yan Shao, Hai Xu, Wei Ji, Jishan Wu, and Kian Ping Loh, “Two-dimensional tessellation by molecular tiles constructed from halogen–halogen and halogen–metal networks,” *Nature Communications* **9**, 4871 (2018).
- [8] Lin Feng, Tao Wang, Zhijie Tao, Jianmin Huang, Guihang Li, Qian Xu, Steven L. Tait, and Junfa Zhu, “Supramolecular Tessellations at Surfaces by Vertex Design,” *ACS Nano* **13**, 10603–10611 (2019).
- [9] Lukáš Kormoš, Pavel Procházka, Anton O. Makoveev, and Jan Čechal, “Complex k-uniform tilings by a simple bitopic precursor self-assembled on Ag(001) surface,” *Nature Communications* **11**, 1856 (2020).
- [10] Marco Polini, Francisco Guinea, Maciej Lewenstein, Hari C. Manoharan, and Vittorio Pellegrini, “Artificial honeycomb lattices for electrons, atoms and photons,” *Nature Nanotechnology* **8**, 625–633 (2013).
- [11] Laura C. Collins, Thomas G. Witte, Rochelle Silverman, David B. Green, and Kenjiro K. Gomes, “Imaging quasiperiodic electronic states in a synthetic Penrose tiling,” *Nature Communications* **8**, 15961 (2017).
- [12] Marlou R. Slot, Thomas S. Gardenier, Peter H. Jacobse, Guido C. P. van Miert, Sander N. Kempkes, Stephan J. M. Zevenhuizen, Cristiane Morais Smith, Daniel Vanmaekelbergh, and Ingmar Swart, “Experimental realization and characterization of an electronic Lieb lattice,” *Nature Physics* **13**, 672–676 (2017).
- [13] Felipe Crasto de Lima and Roberto H. Miwa, “Engineering Metal-spxy Dirac Bands on the Oxidized SiC Surface,” *Nano Letters* **20**, 3956–3962 (2020).
- [14] J. D. Joannopoulos, Pierre R. Villeneuve, and Shanhui Fan, “Photonic crystals: putting a new twist on light,” *Nature* **386**, 143–149 (1997).
- [15] Ming-Hui Lu, Liang Feng, and Yan-Feng Chen, “Phononic crystals and acoustic metamaterials,” *Materials Today* **12**, 34 – 42 (2009).
- [16] Anne S. Meeussen, Erdal C. Oğuz, Yair Shokef, and Martin van Hecke, “Topological defects produce exotic mechanics in complex metamaterials,” *Nature Physics* **16**, 307–311 (2020).
- [17] Alicia J. Kollár, Mattias Fitzpatrick, and Andrew A. Houck, “Hyperbolic lattices in circuit quantum electrodynamics,” *Nature* **571**, 45–50 (2019).
- [18] Hwanmun Kim, Hossein Dehghani, Hideo Aoki, Ivar Martin, and Mohammad Hafezi, “Optical imprinting of superlattices in two-dimensional materials,” *Phys. Rev. Research* **2**, 043004 (2020).
- [19] A. H. Castro Neto, F. Guinea, N. M. R. Peres, K. S. Novoselov, and A. K. Geim, “The electronic properties of graphene,” *Rev. Mod. Phys.* **81**, 109–162 (2009).
- [20] F. Crasto de Lima, Gerson J. Ferreira, and R. H. Miwa, “Tuning the topological states in metal-organic bilayers,” *Phys. Rev. B* **96**, 115426 (2017).
- [21] F. Crasto de Lima, Gerson J. Ferreira, and R. H. Miwa, “Topological flat band, Dirac fermions and quantum spin Hall phase in 2D Archimedean lattices,” *Phys. Chem. Chem. Phys.* **21**, 22344–22350 (2019).
- [22] Xueqin Huang, Yun Lai, Zhi Hong Hang, Huihuo Zheng, and C. T. Chan, “Dirac cones induced by accidental degeneracy in photonic crystals and zero-refractive-index materials,” *Nature Materials* **10**, 582–586 (2011).
- [23] F. Crasto de Lima and G. J. Ferreira, “High-degeneracy points protected by site-permutation symmetries,” *Phys. Rev. B* **101**, 041107 (2020).
- [24] A. Fang, Z. Q. Zhang, Steven G. Louie, and C. T. Chan, “Klein tunneling and supercollimation of pseudospin-1 electromagnetic waves,” *Phys. Rev. B* **93**, 035422 (2016).
- [25] Daniel F. Urban, Dario Bercioux, Michael Wimmer, and Wolfgang Häusler, “Barrier transmission of Dirac-like pseudospin-one particles,” *Phys. Rev. B* **84**, 115136 (2011).
- [26] Zhicheng Rao, Hang Li, Tiantian Zhang, Shangjie Tian, Chenghe Li, Binbin Fu, Cenyao Tang, Le Wang, Zhilin Li, Wenhui Fan, Jiajun Li, Yaobo Huang, Zhehong Liu, Youwen Long, Chen Fang, Hongming Weng, Youguo Shi, Hechang Lei, Yujie Sun, Tian Qian, and Hong Ding, “Observation of unconventional chiral fermions with long Fermi arcs in CoSi,” *Nature* **567**, 496–499 (2019).
- [27] Chenguang Fu, Tiejun Zhu, Yanzhong Pei, Hanhui Xie, Heng Wang, G. Jeffrey Snyder, Yong Liu, Yintu Liu, and Xinbing Zhao, “High Band Degeneracy Contributes to High Thermoelectric Performance in p-Type Half-Heusler Compounds,” *Advanced Energy Materials* **4**, 1400600 (2014).
- [28] Menghao Wu, Zhijun Wang, Junwei Liu, Wenbin Li, Huahua Fu, Lei Sun, Xin Liu, Minghu Pan, Hongming Weng, Mircea Dincă, Liang Fu, and Ju Li, “Conetronics in 2D metal-organic frameworks: double/half Dirac cones and quantum anomalous Hall effect,” *2D Materials* **4**, 015015 (2016).
- [29] Titus Neupert, Luiz Santos, Claudio Chamon, and Christopher Mudry, “Fractional Quantum Hall States at Zero Magnetic Field,” *Phys. Rev. Lett.* **106**, 236804 (2011).
- [30] Jia-Xin Yin, Songtian S. Zhang, Guoqing Chang, Qi Wang, Stepan S. Tsirkin, Zurab Guguchia, Biao Lian, Huibin Zhou, Kun Jiang, Ilya Belopolski, Nana Shumiya, Daniel Multer, Maksim Litskevich, Tyler A. Cochran, Hsin Lin, Ziqiang Wang, Titus Neupert, Shuang Jia, Hechang Lei, and M. Zahid Hasan, “Negative flat band magnetism in a spin-orbit-coupled correlated kagome magnet,” *Nature Physics* **15**, 443–448 (2019).
- [31] Yuan Cao, Valla Fatemi, Shiang Fang, Kenji Watanabe, Takashi Taniguchi, Efthimios Kaxiras, and Pablo Jarillo-Herrero, “Unconventional superconductivity in magic-angle graphene superlattices,” *Nature* **556**, 43–50 (2018).
- [32] Leon Balents, Cory R. Dean, Dmitri K. Efetov, and Andrea F. Young, “Superconductivity and strong correlations in moiré flat bands,” *Nature Physics* **16**, 725–733 (2020).
- [33] Toshihiko Baba, “Slow light in photonic crystals,” *Nature Photonics* **2**, 465–473 (2008).